Environ. Sci. Technol. **1995**, *29*, 363–371

Sorption of Benzo[*a*]pyrene and Phenanthrene on Suspended Harbor Sediment as a Function of Suspended Sediment Concentration and Salinity: A Laboratory Study Using the Cosolvent Partition Coefficient

WIM J. M. HEGEMAN,* CORNELIS H. VAN DER WEIJDEN, AND J. P. GUSTAV LOCH

Department of Geochemistry, Institute of Earth Sciences, Utrecht University, P.O. Box 80.021, 3508 TA Utrecht, The Netherlands

The sorption of benzo[*a*]pyrene (BaP) and phenanthrene (PHE) on sediment collected in the harbor of Rotterdam was studied in batch experiments using ^{14}C-labeled compounds. In order to simulate various estuarine conditions, we investigated the effects of various sediment concentrations and salinities on sorption of these compounds. We determined the apparent partitioning as well as the cosolvent partitioning between the liquid and solid phases. The apparent partition coefficient (K_p^{App}) is influenced by the presence of colloids and dissolved organic matter. The influence of these components is minimized by the use of the cosolvent method in which the partition coefficient (K_p*) is determined by extrapolation of the partition coefficients obtained in a variety of solutions with water and methanol. The effect of sediment concentration on sorption was investigated at five different sediment concentrations ranging from 0.064 to 10.8 g/L. In contrast to K_p*, K_p^{App} was found to be sensitive to the sediment concentration. Log K_p* (with K_p* in L/kg), determined for different sediment concentrations, was 5.2–6.3 for BaP and 2.8–3.6 for PHE, whereas log K_p^{App} was 4.1–5.6 for BaP and 2.9–4.0 for PHE. The salt concentration was varied with dilutions of Milli-Q water and seawater; the salinity ranged from 0 to 35. The influence of salinity on K_p* was small; the increase in log K_p* from freshwater to seawater is approximately 0.2 for BaP and 0.1 for PHE.

Introduction

Sediments deposited in Rotterdam Harbor contain a wide variety of organic contaminants, including polycyclic aromatic hydrocarbons (PAHs) such as benzo[*a*]pyrene (BaP) and phenanthrene (PHE). These sediments are often resuspended, either by dredging activities or by natural resuspension. Suspended sediments in estuaries are usually subject to changing salinity conditions. In order to elucidate the fate of PAHs under estuarine conditions, laboratory sorption experiments were carried out in which sediment concentration and salinity were varied.

In sorption experiments, the solid and liquid phases are usually separated to determine the partitioning of a hydrophobic organic compound (HOC). This situation is illustrated in Figure 1. An HOC in the aquatic environment is distributed between the solid and the liquid phase. The liquid phase consists of three sub-phases: the truly aqueous solution, a dissolved organic matter (DOM) fraction, and colloids. Because of their high specific surface area, colloidal particles may acquire a high HOC content. Removal of the colloidal size particles depends on the centrifugal force in the centrifuge tube or on the pore diameter when a filter is used. DOM also has a high affinity for HOCs. Both types of association result in a higher apparent solubility of HOCs in the liquid phase. The method of separation, which is operationally defined, determines the apparent partition coefficient (K_p^{App}) of the HOC. Due to the presence of DOM and colloids, K_p^{App} will be lower than the true K_p. The true K_p is defined as the ratio between the concentration of the HOC in the solid phase and the concentration in the true aqueous solution. The difference between K_p^{App} and K_p can be measured by using the cosolvent partition method. This method uses partition coefficients determined at various cosolvent–water mixtures which are subsequently extrapolated to 0% cosolvent. The method is described in more detail in the next section.

The effect of sediment concentration on the partition coefficient has been demonstrated by several authors (*1*–*6*). These studies have shown that the apparent partition coefficient and the sediment concentration are inversely related. Several theories have been put forward to explain the observations, namely, (1) the existence of a colloidal phase, (2) particle interactions, (3) increasing aggregation at high particle concentration (*7*). But no thermodynamic explanation could be given for the sediment concentration effect.

This study was performed to determine the effect of sediment concentration and salinity using the apparent partition coefficient K_p^{App} and the cosolvent partition coefficient (K_p*). The cosolvent partition coefficient (K_p*) is considered to be the best estimate of the true partition coefficient and was therefore used to estimate the sorption behavior of BaP and PHE.

Theory

Equilibrium sorption of HOCs on suspended solid matter in an aqueous phase is usually described with a linear

* To whom correspondence should be addressed; e-mail address: whegeman@earth.ruu.nl; Fax: +3130535030.

0013-936X/95/0929-0363$09.00/0

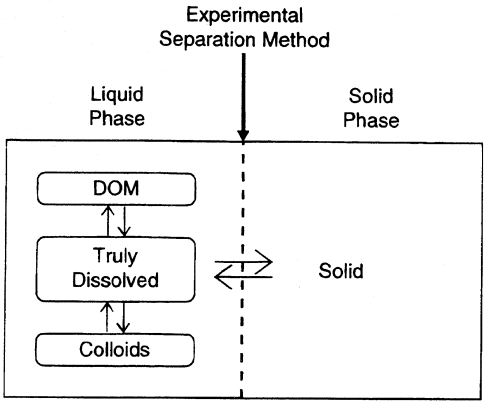

FIGURE 1. Schematic representation of the partitioning of a hydrophobic compound between the liquid phase and the solid phase. The total hydrophobic compound concentration in the liquid phase is subdivided into the concentration in the true dissolved phase, the DOM associated phase, and the colloid associated phase.

sorption isotherm (*8–11*). The slope of the isotherm is the partition coefficient K_p (L/kg), which is the ratio of the concentration of an HOC in the solid C_s (kg/kg of solid matter) and its concentration in the water solid phase C_w (kg/L of water) at equilibrium:

$$K_p = C_s/C_w \tag{1}$$

In eq 1, the concentration in the water phase is the dissolved concentration excluding associations with colloids and DOM. The partition coefficients of HOCs correlate well with the organic matter content of the solid phase and can be normalized on the organic carbon fraction in the sediment (f_{oc}), K_{oc} being the normalized partition coefficient:

$$K_{oc} = K_p/f_{oc} \tag{2}$$

The experimentally observed concentration of an HOC in the water phase is operationally defined. This apparent concentration C'_w consists of a component in true solution, a component associated with DOM (*12–14*) and a component associated with colloidal particles. C'_w can therefore be expressed as the sum of these components:

$$C'_w = C_w + C_{DOM} + C_{Coll} \tag{3}$$

where C'_w is the apparent concentration of the HOC in water (kg/L of water); C_w is the true concentration in water (kg/L of water); C_{DOM} is the component of the apparent concentration associated with DOM (kg/L of water); and C_{Coll} is the component of the apparent concentration associated with colloids (kg/L of water).

It can be derived that, analogous to eq 1, an apparent partition coefficient can be calculated from

$$K_p^{App} = \frac{C_s}{C'_w} = \frac{C_s}{C_w(1 + K_{DOM}C_{DOM}^* + K_{Coll}C_{Coll}^*)} \tag{4}$$

where K_p^{App} is the apparent partition coefficient (L/kg); K_{DOM} is the partition coefficient between DOM and water (L/kg of DOM); C_{DOM}^* is the concentration of DOM in water (kg of DOM/L); K_{Coll} is the partition coefficient between colloids and water (L/kg of colloid); C_{Coll}^* is the the concentration of the colloids in water (kg colloid/L).

Substitution of the true partition coefficient (eq 1) into eq 4 will give

$$K_p^{App} = \frac{K_p}{(1 + K_{DOM}C_{DOM}^* + K_{Coll}C_{Coll}^*)} \tag{5}$$

When the contribution of both DOM and colloids is reduced, the apparent partition coefficient (eq 5) will approach the true partition coefficient.

The cosolvency theory has been developed from the concept of solubility in mixed solvents (*15, 16*). The partition of an HOC between solid phase and liquid phase in mixed solvents can be expressed as (*17–20*)

$$\log K_{p,m}^{App} = \log K_p - \alpha\sigma z \tag{6}$$

where $K_{p,m}^{App}$ is the apparent partition coefficient in mixed solvents (L/kg); K_p is the true partition coefficient in water (L/kg); $\alpha\sigma$ is the slope of the plot log $K_{p,m}^{App}$ versus z (–); z is the volume fraction of the cosolvent (–); σ represents the effect of the cosolvent on the solute solubility; and α relates the activity coefficient of the HOC in water to the activity coefficient in the solid phase (*20*).

In eq 6, K_p and $K_{p,m}^{App}$ are expressed in liter per kilogram. The number of moles of solvent is not constant at different water/cosolvent ratios. Therefore, the experimentally determined partition coefficients to be extrapolated must be in moles of solvent per kilogram. Equation 6 thus changes into

$$\log\left[K_{p,m}^{App}\left(\frac{\frac{V_{water}}{q_{water}} + \frac{V_{cosolvent}}{q_{cosolvent}}}{V_{Total}}\right)\right] = \log\left(K_p\frac{1}{q_{water}}\right) - \alpha\sigma z \tag{7}$$

where $V_{water,cosolvent}$ is the volume of water or cosolvent (L); V_{Total} is the total volume of water and cosolvent (L); and $q_{water,cosolvent}$ is the molar volume of water or cosolvent (L/mol).

For convenience, eq 7 can be rewritten as

$$\log \dot{K}_{p,m}^{App} = \log \dot{K}_p - \alpha\sigma z \tag{8}$$

According to eq 8, the apparent partition coefficient in mixed solvents decreases in a log-linear fashion with increasing volume fraction (z) of the cosolvent. Log $\dot{K}_p$ can be obtained by extrapolating the plot of log $\dot{K}_{p,m}^{App}$ (mole/kg) against z. When multiplied by the molar volume of water, $\dot{K}_p$ is transformed to K_p^* (L/kg). Unless specified, K_p^* will hereafter be referred to as the cosolvent partition coefficient.

Now that a cosolvent partition coefficient has been defined, the terms in eqs 4 and 5 can be reconsidered. When an HOC-containing sediment is suspended in water, the major part of the HOC remains in the solid phase. The apparent dissolved concentration, and subsequently the apparent partition coefficient of the HOC ($K_{ow} > 10^5$), is assumed to be primarily determined by its concentration on both the colloids and DOM (*21, 22*). With the addition of the cosolvent, C'_w (eq 4) will increase at the expense of C_s on the assumption that there has been no change in the contribution of colloids and DOM to C'_w. A DOM contribution to C'_w is not likely because sediment cross-linked polymer particulate organic matter is not readily soluble in the solvent mixture (*20, 23*). As the mole fraction of the cosolvent in the mixture increases, more HOC will be

TABLE 1

Concentrations in Harbor Sediment

sediment	phenanthrene (μg/kg)	benzo[*a*]pyrene (μg/kg)	organic carbon (%)
Rotterdam Harbor	658	570	4.60

dissolved. The role of the cosolvent then out-weighs the role of colloids and DOM. By extrapolation of the cosolvent concentration to zero, the apparent partition coefficient will approach the true partition coefficient K_p (eq 1).

The solubility and the partition coefficient of an HOC depend on the salt concentration (*24, 25*). This dependency, shown as a partition coefficient, is expressed as a modification of an equation of Chin and Gschwend (*22*):

$$\log K_{oc}^* = \log K_{oc}^*(sw) + aK_sC_{Sal} - b \qquad (9)$$

where K_{oc}^* and $K_{oc}^*(sw)$ are the organic carbon-normalized partition coefficients in the salinity gradient and extrapolated for seawater respectively (L/kg of organic carbon); a is an empirical constant; K_S is the Setschenow constant (L/mol) [K_S (BaP), 0.333 L/mol and K_S (PHE), 0.275 L/mol (*26*)]; C_{Sal} is the molar salt concentration based on NaCl (seawater $\approx$ 0.6 M); and b is an empirical constant, representing the calculated difference between log K_{oc}^* for freshwater and for seawater. Equation 9 was used to calculate the salinity effect of the HOCs on the partition coefficients.

Materials and Methods

Sediment. Harbor sediment from the Waalhaven in Rotterdam was collected with a 50-L sediment grab. The sampling site was chosen as being representative of the average sediment, which is not in contact with North Sea water but may easily be resuspended and transported to the open sea (salinity at sampling site: 0 g kg^{-1} or ‰). The silty sediment was wet-sieved (<63 μm) to remove coarse particles. In this sediment, PHE and BaP were analyzed according to the method described by Van Zoest and Van Eck (*27*). The organic carbon content, based on dry weight, was measured by total combustion of the carbonate-free sediment with oxygen. After separation of water and oxygen the total carbon dioxide pressure was measured, and the organic carbon content in the sediment was calculated. The result is given in Table 1.

Solutions with salinities of 0, 2.5, 5, 10, 20, and 35‰ were prepared by dilutions of uncontaminated North Atlantic Ocean water (S = 35‰) with Milli-Q water (Millipore).

Methanol. HPLC-grade methanol (Westburg, Leusden, NL) was used in all experiments.

PAH Standards. Benzo[*a*]pyrene and phenanthrene standards were used as carriers and had a purity of 99.9% (Promochem, Wesel, FRG).

Radiotracers. [7−10-^{14}C]Benzo[*a*]pyrene (Amersham, Den Bosch, NL; specific activity, 2.16 GBq/mmol) with a chemical purity of >98% was used. This radiolabel was eluted over a C_{18} column (0.5 g of SPE, J. T. Baker, Deventer, NL) with a water/acetonitrile gradient ranging from 0% to 100% acetonitrile. The elution fractions were collected, and the elution fraction with the highest β-activity was used in the experiments. The purity was confirmed with gradient elution on RP-HPLC (Hewlett Packard) followed by β-counting. No activity peaks other than the peak of ^{14}C-BaP were observed.

TABLE 2

Sampling Scheme in Each Sorption Vessel for Various Suspension Concentrations and Various Salinities[a]

suspension concn (g/L)	phase to be analyzed
0	C_L, C_{Wall}
0.064	C_L, C_s, C_{Wall}
0.53	C_L, C_s, C_{Wall}
1.08	C_L, C_s, C_{Wall}
5.46	C_L, C_s, C_{Wall}
10.8	C_L, C_s, C_{Wall}

[a] For every combination of salinity and suspension concentration, eight separate vials are needed for different MeOH/water (v/v) solutions (0, 10, 20, 30, 40, 50, 60, 100% MeOH/water). Salinity of 0, 2.5, 5, 10, 20, or 35‰. C_L is the liquid phase; C_s is the solid phase; C_{Wall} is the vessel wall.

[9-^{14}C]Phenanthrene (specific activity, 0.48 GBq/mmol; Sigma, St.Louis, MO) had an HPLC-certified radioactive purity of 99.4%; therefore this compound was not purified.

The PAH standards were mixed with the radiotracer and methanol (HPLC-quality) to give stock solutions of BaP (0.31 mmol/L) and PHE (0.30 mmol/L) in methanol. These stock solutions were added to the vessels in which the sorption experiments were carried out. The added PAH concentrations were at least 2 orders higher than in the harbor sludge so that isotopic exchange would not interfere with the sorption experiments.

Sorption. Solutions of volume fractions of methanol (0, 10, 20, 30, 40, 50, 60, 100%) and water (salinities = 0, 2.5, 5, 10, 20, 35) were made in glass Erlenmeyers with glass-ground stoppers to prevent volatilization of MeOH. An amount of 1.5 mL was pipetted into 1.7 mL glass HPLC sample vials, and 0.1 mL of five different suspension concentrations was added to the various vials. The suspension concentrations in the vials are given in Table 2. To these suspensions, 25 μL of either PHE or BaP stock solution was added using an HPLC injection syringe. The vials were closed with a screw-cap sealed with Teflon liner. The sediment was kept in suspension by axial rotation of the vial at a slow speed ($\pm$ 60 rpm) in the dark and at 21 °C. Preliminary kinetic studies showed that sorption was complete within 14 days. Biotransformation of the PAHs was negligible during this period (*28, 29*), especially when a quantity larger than 10% MeOH was added (*30*).

After 14 days, the suspended matter and the solution were separated by centrifugation for 15 min at 4000*g*. An amount of 800 μL of the clear solution was siphoned off with a glass Pasteur pipet that was connected to a volumetric pipet (80−2000 μL) and directly injected into the scintillation vials.

For the determination of the PAHs in the solid phase, the residue in the vial was resuspended, and the suspension (800 μL) was removed to 10-mL glass vials containing 5 mL of MeOH. An amount of 800 μL of Milli-Q water was added to the 1.7-mL vial, which was then shaken vigorously to resuspend any sediment particles left on the wall of the vial. This was also added to the 10-mL vial. The 10 mL vial was capped and rotated for 2 h. After this extraction with MeOH, the vials were centrifuged (4000*g*), and 0.8 mL of the supernatant was pipetted into a scintillation vial. This

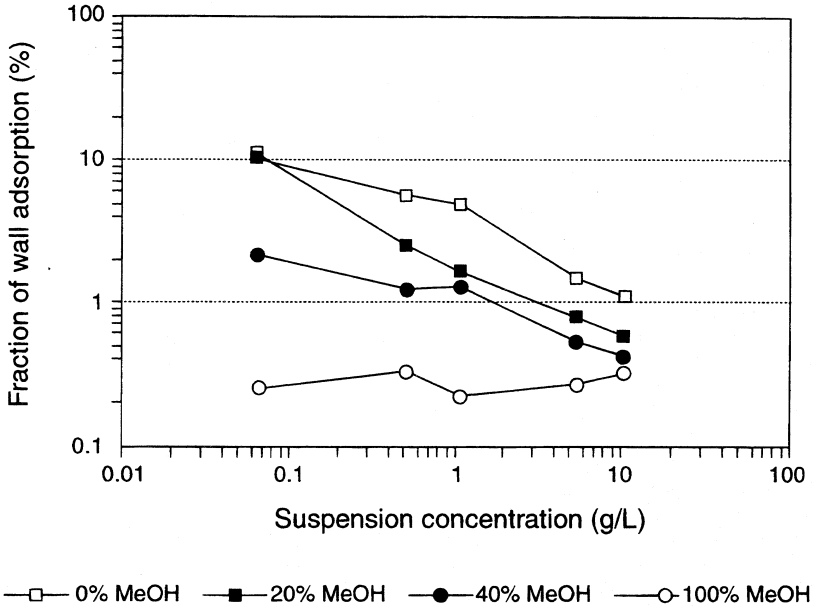

FIGURE 2. Fractions of benzo[*a*]pyrene adsorbed on the wall of the reaction vials as a function of suspension concentration for four different volume fractions of MeOH. Average values for different salinities are presented.

extraction procedure is used to prevent the radiolabel from being quenched by particles in an LSC cocktail. To determine the adsorption onto the vessel wall, 0.8 mL of MeOH was added to the empty vial. The vial was rotated for 2 h, and its content was then pipetted into scintillation vials.

The sampling scheme is given in Table 2. For each salinity level and each suspension concentration, eight separate vials were needed for the different MeOH/water dilutions. A total number of 576 separate vials were sampled for either PHE or BaP. For each vial, three phases (water, sediment, and wall) were analyzed.

Liquid Scintillation Counting (LSC). The scintillation vials contained 10 mL of scintillation cocktail (Safety Cocktail, J. T. Baker, Deventer, NL). After the added aliquots of the solutions had been mixed with the cocktail, β-counting was carried out with a Packard (minimaxiB, Tricarb 1000 Series) counter. The ^{14}C activity was counted using an energy channel ranging from 0 to 156 keV and calibrated against a Packard standard background vial. The samples were counted until a 0.5% counting error was attained. An efficiency curve was made with five standard 1.67 kBq of ^{14}C-labeled quench vials (Packard), and the activities of the samples were compared to the ^{226}Ra (0.37 MBq) external source. The efficiency of all the samples was between 92 and 93%, which indicates that no additional quenching had occurred as a result of the added liquid. Since the measured activity was related to the initial added concentration (25 μL of stock solution) of the PAH compounds, it was possible to calculate the concentrations and partitioning.

Partition Coefficients. The apparent partition coefficient in various mixed solvents ($K_{p,m}^{App}$) was calculated as the measured activity in the solid phase (A_S) divided by the activity in the liquid phase (A_L) and the suspension concentration (m):

$$K_{p,m}^{App} = A_S/A_L m \quad (10)$$

The cosolvent partition coefficient, based on methanol as a cosolvent, was calculated according to eq 8 and extrapolated linearly to 0% MeOH. The $\dot{K}_p$ value in mole per kilogram was converted to K_p^* (L/kg) by multiplication by the molar volume of water q_{water}. The molar volumes used are as follows: $q_{water} = 0.01805$ L/mol and $q_{cosolvent(MeOH)} = 0.04049$ L/mol.

Results and Discussion

Application of Cosolvent Partition Coefficient. In Figure 2, adsorption of BaP on the vessel wall is shown for various suspended sediment concentrations. The adsorption on the vessel wall plays a role in sorption experiments at low sediment concentrations and in experiments where no MeOH was added. The adsorption on the vessel wall at 100% MeOH is negligibly low for all sediment concentrations. In most experiments, the wall adsorption is less than 2% of the initial addition. For the extrapolation to the cosolvent partition coefficient, only MeOH volume fractions ≥20% were used. It can be concluded that wall adsorption plays only a minor role in our experiments. Analogous calculations were performed for PHE. The wall adsorption for PHE was in all cases less than for BaP because of the less hydrophobic character of PHE.

In Figure 3, the percentage of the initial addition of BaP in the three compartments analyzed are plotted versus the volume fraction of methanol. The total recovered addition is calculated by summation of the fractions. Figure 3 shows that the fraction in the solid phase decreases with increasing volume fraction of MeOH. When the volume fraction of MeOH was between 0 and 20%, the solid phase concentration of BaP hardly changed, but when the volume fraction of MeOH exceeded 20%, the fraction of BaP decreased in the solid phase and increased in the liquid phase. When the fraction of MeOH was ≥60%, the fraction of BaP in the

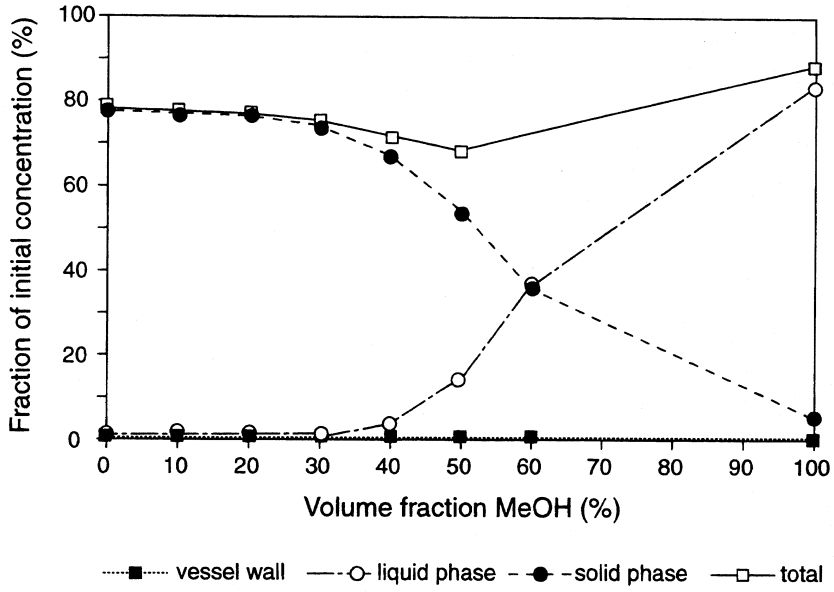

FIGURE 3. Fractions of the initial addition of benzo[*a*]pyrene in three compartments analyzed, and the sum of the fractions in these compartments as a function of volume fraction of methanol in the liquid phase. Salinity = 35‰; suspension concentration = 10.8 g/L.

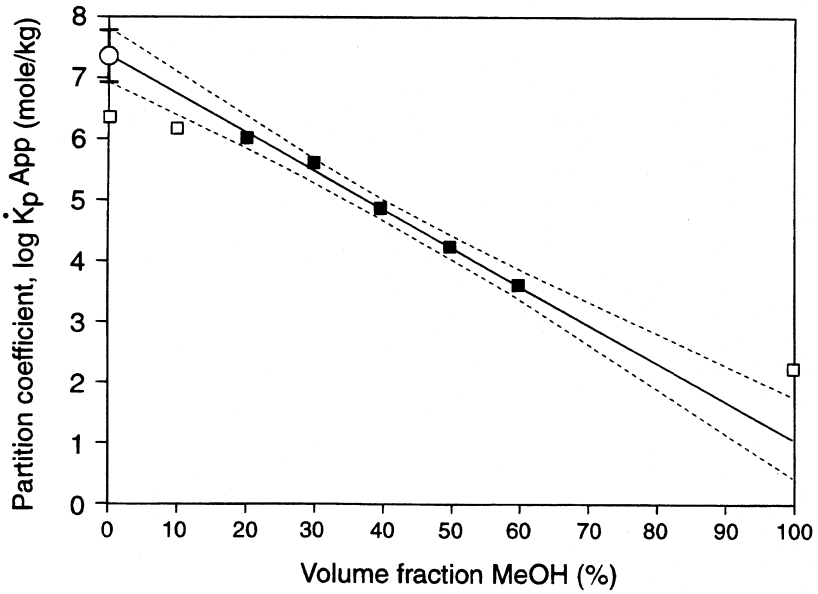

FIGURE 4. Apparent partition coefficient (mol/kg) of benzo[*a*]pyrene as a function of volume fraction methanol with 95% confidence intervals ($S = 35‰$, $m = 10.8$ g/L). The intercept with the *y*-axis gives the cosolvent partition coefficient $\dot{K}_p$ (open circle). The 95% confidence interval at this point is given by an error bar. The filled squares denote the apparent partition coefficients used for the linear regression. The open squares are apparent partition coefficients not used in the regression.

solid phase will be depleted. Preliminary studies showed that when the MeOH fraction was between 70 and 100% the cosolvent method could not be used. The total amount measured in the three compartments is never equal to the amount added because there are always losses due to experimental handling. For all experiments with BaP and PHE the recovery ranged from 75% to 95% of the initial addition. For every volume fraction of MeOH, the apparent partition coefficient was calculated on the basis of measured concentrations in the solid and liquid phases.

In Figure 4, the apparent partition coefficients are plotted versus the volume fraction of methanol for one suspension concentration (10.8 g/L) and one salinity ($S = 35‰$). The cosolvent partition coefficient ($\dot{K}_p$) is obtained by extrapolation of the apparent partition coefficients for mixed solutions in the range 20–60% MeOH, applying a least-squares fitting method. When z is between the 20 and 60% MeOH, the extrapolation of the log $\dot{K}_{p,m}^{App}$ gives the best linear relation. The sediment will be depleted when the

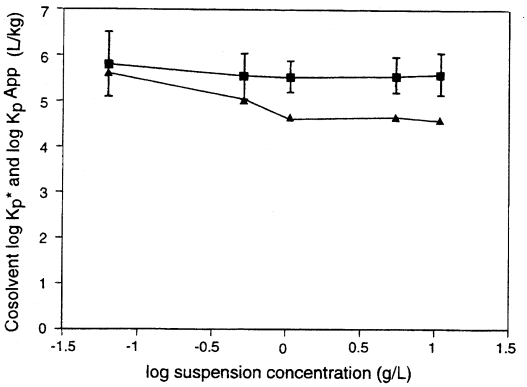

FIGURE 5. Cosolvent partition coefficient (■) and the apparent partition coefficient at 0% MeOH (▲) of benzo[*a*]pyrene versus the suspension concentration in seawater (S = 35‰). The error bars represent the statistical 95% confidence interval. (▲) represents single measurements.

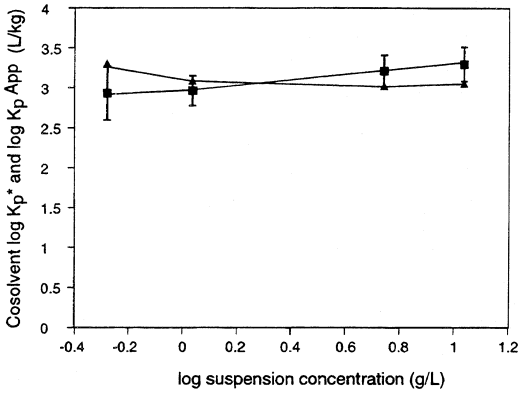

FIGURE 6. Cosolvent partition coefficient of phenanthrene (■) and the apparent partition coefficient (▲) versus the suspension concentration in seawater (S = 35‰). The error bars represent the 95% confidence interval. (▲) represents single measurements.

volume fraction of MeOH is above 60%, whereas association of the HOC with DOM and colloids is important when MeOH is <20%. The difference between the cosolvent partition coefficient (open circle) and the apparent partition coefficient (open square), as shown in Figure 4 at 0% MeOH, is attributed to the contributions of BaP bound to colloids and to the contribution of DOM to the total dissolved BaP concentration. For the cosolvent partition coefficient, the 95% error interval is given. This interval shows the maximum error for reliable cosolvent partition coefficients. A similar extrapolation was performed for each set of batch experiments. To obtain a cosolvent partition coefficient, five partition coefficients are required for the regression. When fewer partition coefficients are used for extrapolation, the statistical errors will be too large. All linear regression lines have a high correlation coefficient and are highly significant.

When the cosolvent partition method is used as a standard technique, the number of samples can be reduced because the shape of the curve of the apparent partition coefficient as a function of the volume fraction of MeOH is known. Therefore, a less laborious determination with only 2 volume fractions of cosolvent, for example, at 20% and at 60% volume fraction of MeOH, could be used for the extrapolation to obtain the cosolvent partition coefficient.

The parameter σ (eq 7) is determined with the experiments where no suspension was added. In these experiments, an additional effect of either DOC, colloids, or interactions with the suspended sediments on the partitioning is not present; K_p^{App} represents the partitioning with the glass wall; and the slope represents σ. Then the nonsolubility enhancement expressed as a lumped parameter α is calculated by $\alpha = \alpha\sigma/\sigma$. α was between 0.7 and 0.8 for PHE and between 0.9 and 1 for BaP. These values are in agreement with those of Walters and Guiseppi-Elie (*31*). It is not clear how the solid organic matrix is affected by the concentration of the cosolvent. A change in the spacial orientation of the organic matrix may provide sorption sites which were not available before (*32, 33*).

Effect of Suspended Solid Concentration. In Figure 5, both the cosolvent partition coefficient and the apparent partition coefficient at 0% MeOH for BaP are plotted versus the suspension concentration. The cosolvent partition coefficient has an almost constant value, whereas the apparent partition coefficient decreases when the concentration of the suspension increases.

In Figure 6, the cosolvent partition coefficient (K_p*) and the apparent partition coefficient (K_p^{App}) for PHE are plotted against the sediment concentration. For this salinity (S = 35‰), an effect of suspended sediment concentration on the K_p* of PHE is still present, but the slope has changed sign. Relative constant values of the slope were obtained at other salinities. The slopes of these double-logarithmic plots of BaP and PHE are listed in Table 3. The slope indicates the sensitivity of the partition coefficient to changing suspension concentration. For both compounds, at nearly all salinities, the slope of K_p^{App} has a higher absolute value than the slope of K_p*. This means that K_p* is less dependent on the sediment concentration than is K_p^{App}.

The significance levels for the regression are high because the cosolvent partition coefficient is derived from an extrapolated value with a relatively high inaccuracy. It indicates that the partition coefficient is practically independent of sediment concentration. This observation has major advantages for sorption studies and for prediction studies of HOC in estuaries. Any residual effect of suspension concentration on K_p* may be attributed to particle–particle aggregation.

Salinity Effect. In Figure 7, the cosolvent partition coefficient of BaP is shown as a function of salinity (lower line) for one sediment concentration (10.8 g/L) with the 95% error intervals. The partition coefficient increases slightly from freshwater to seawater. The data points connected by the upper line represent the cosolvent partition coefficient normalized on organic carbon content (K_{oc}*) calculated from K_p* (K_{oc}* = K_p*/f_{oc}). According to eq 9, the effect of salt concentration is shown as a linear least-squares fitted model (Figure 7). The errors in both log K_p* and log K_{oc}* are the same. A slight increase in K_{oc}* is observed with increasing salinity.

Figure 8 shows K_p* of PHE and K_{oc}* versus salinity. The same linear model was used. For PHE, a small increase in K_{oc}* is observed when the salinity increases. In Table 4, the effect of increasing salinity on BaP and PHE sorption is shown for all suspension concentrations. With decreasing suspension concentrations, the effect of salinity is less for BaP. For PHE hardly any salinity effect could be observed (Figure 8), as indicated by a low b value (Table 4). A possible explanation is the less hydrophobic properties of PHE. For

TABLE 3

Slope of Logarithm of Cosolvent Partition Coefficient (K_p*) and Apparent Partition Coefficient (K_p^{App}) versus Logarithm of Sediment Concentrations for Benzo[*a*]pyrene and Phenanthrene at Different Salinities

	benzo[*a*]pyrene		phenanthrene	
salinity	slope ± SE[a] (log K_p*)	slope ± SE (log K_p^{App})	slope ± SE (log K_p*)	slope ± SE (log K_p^{App})
0	−0.45 ± 0.15	−0.44 ± 0.06	−0.004 ± 0.01	−0.37 ± 0.09
2.5	−0.36 ± 0.09	−0.44 ± 0.08	0.026 ± 0.14[b]	−0.12 ± 0.02
5	−0.19 ± 0.10[b]	−0.38 ± 0.08	0.007 ± 0.11[b]	−0.30 ± 0.05
10	−0.17 ± 0.11[b]	−0.40 ± 0.12	−0.11 ± 0.18[b]	−0.25 ± 0.03
20	−0.30 ± 0.16[b]	−0.41 ± 0.09	−0.04 ± 0.15[b]	−0.48 ± 0.12
35	−0.08 ± 0.05[b]	−0.46 ± 0.12	0.31 ± 0.02	−0.15 ± 0.08

[a] The standard error (SE) of the slope is calculated with a least-squares fitted method. [b] Significance levels for regression were on a 10% level ($P < 0.1$) or less significant ($P > 0.1$).

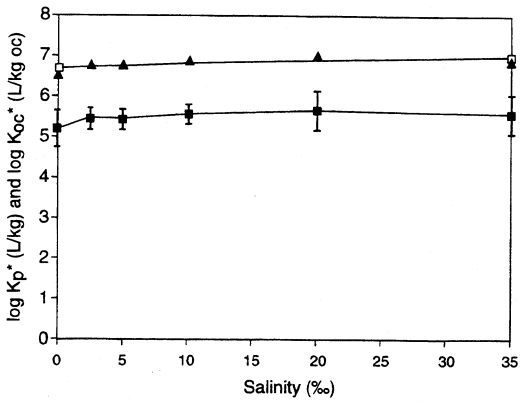

FIGURE 7. Cosolvent partition coefficient (K_p*) and the cosolvent partition coefficient normalized on organic carbon (K_{oc}*) of benzo[*a*]pyrene as a function of salinity (m = 10.8 g/L). The filled squares represent log K_p*, and the filled triangles represent the log K_{oc}* values. The error bars represent the 95% confidence interval of the cosolvent partition coefficient. The open squares at S = 0‰ and at S = 35‰ represent the calculated log K_{oc}* value in freshwater and seawater, respectively. The regression line represents log K_{oc}* versus salinity calculated with a least-squares fitting method according to eq 9.

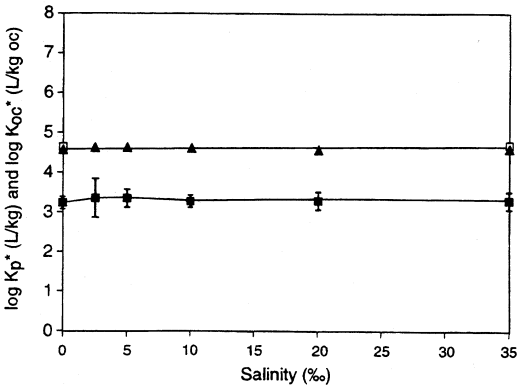

FIGURE 8. Cosolvent partition coefficient (K_p*) and the organic carbon normalized partition coefficient (K_{oc}*) of phenanthrene as a function cosolvent of salinity (m = 10.8 g/L). Additional information similar to that given in Figure 7.

low suspension concentrations, hardly any dependence of salinity is observed for BaP. This is indicated by the low value of both b and a (except m = 0.064). The relatively high error of log K_p* has an effect on the significance levels of the regression and on the prediction of the salinity effect. As the best available experimental techniques were applied, it is difficult to reduce the error in the partition determination. Therefore, changes in log K_{oc}* due to salinity are negligible according to this technique.

TABLE 4

Parameters for Dependence of Organic Carbon Normalized Cosolvent Partition Coefficient (K_{oc}*) on Salinity[a]

	benzo[*a*]pyrene			phenanthrene		
sediment concentration	log K_{oc}*(sw)	*a*	*b*	log K_{oc}*(sw)	*a*	*b*
10.8	7.02	1.56	0.31	4.64	0.22	0.036
5.46	7.00	1.89	0.38	4.62	1.32	0.22
1.08	6.83	0.20	0.040	4.24	−0.52	−0.087
0.53	6.92	0.51	0.10	4.32	0.64	0.11
0.064	7.26	−1.07	−0.21	5.10[b]	3.06[b]	0.50[b]

[a] Expressed as C_{Sal}, the molar salt concentration based on NaCl, according to log K_{oc}* = log K_{oc}*(sw) + $aK_SC_{Sal} - b$ with K_S = 0.333 L/mol (BaP) and K_S = 0.275 L/mol (PHE). Log K_{oc}*(sw) denotes the calculated organic carbon normalized cosolvent partition coefficient at S = 35‰. a and b are empirical constants. b indicates the difference of log K_{oc}* at C_{Sal} = 0.6 (seawater) and C_{Sal} = 0 (freshwater), whereas a denotes the slope of log K_{oc}* versus K_SC_{Sal}. The parameters are calculated for different suspension concentrations with a least-squares fitting method. For the calculations, n = 6 unless specified otherwise. In all experiments, significance levels were high ($P > 0.1$). [b] Calculated with n = 5.

The extrapolated log K_{oc}*(sw) for BaP is relatively constant for all sediment concentrations. The value of b (eq 9) lies between 0.3 and 0. This value is in accordance with the one observed by Chin and Gschwend (*22*).

Salts can change the compressibility of water more than nonelectrolytes, and this compressibility changes in a logarithmic way with the salt concentration (*34, 35*). This can be attributed to an enhancement of the arrangement of the water molecules. Therefore, the addition of salt to an aqueous nonelectrolyte solution results in a decrease in the solubility of the nonelectrolyte (salting out). The hydration of salt ions causes electrostriction of the water solution and expels the HOC molecules from the water (*36*). The theory of the salt effect predicts an increase in the partition coefficient with increasing salt concentration, but this is not evident from our results.

The organic carbon normalized cosolvent partition coefficient shows a constant value at salinities equal to seawater (S = 35‰). Table 4 shows for all suspended sediment concentrations a constant value of log K_{oc}*(sw) for BaP (7.0 L/kg) and PHE (4.5 L/kg). This indicates that

one value for the partition coefficient may be used for all sediment concentrations.

Field Studies. Laboratory experiments can elucidate natural estuarine processes, but complicated estuarine processes like resuspension at high turbidity can overrule specific sorption processes (*37*). Our results give an indication that K_{oc}* in laboratory experiments slightly increases from freshwater to sea water. This effect was not shown for partition coefficients of HOC normalized on organic carbon derived from field studies in estuaries (*27, 38*). In the Rhine and Scheldt Estuary, a decrease in HOC in the solid concentration in an estuarine environment was attributed to the mixing of riverine and marine particles: particulate PAHs behaved conservatively in the estuaries. No increase in the partition coefficient with salinity could be determined. Future sorption studies will require fine-tuning of the measurements in order to specify changes in the partition coefficient occurring due to the salt concentration.

Major temperature effects on sorption were shown by Bergen et al. (*39*). In their statistical analysis, the temperature had a major effect on the partitioning of HOCs, whereas the total suspended solids concentration had only a minor influence on the partition coefficient. These studies show that future sorption studies will have to take a multiplicity of factors into account, not only salinity and sediment concentration.

Conclusions

The sorption behavior of two hydrophobic organic compounds, benzo[*a*]pyrene (BaP) and phenanthrene (PHE), was studied with batch techniques to elucidate the influence of sediment concentration and salinity. A distinction was made between the apparent partition coefficient (K_p^{App}) and the cosolvent partition coefficient (K_p*). K_p* represents the true partition coefficient, i.e., the concentration ratio between the solid phase and the water phase. According to the cosolvent theory, the use of a cosolvent coefficient can overrule influences of colloids and DOM. Therefore, the cosolvent method will make it possible to solve separation problems which will be encountered when partioning occurs between the solid and liquid phase. At different suspended sediment concentrations, K_p* showed a constant value for BaP and therefore eliminates influences attributed to DOM and colloids. For both BaP and PHE, K_p* indicated a slight increase when salinity was increased from freshwater to seawater.

Acknowledgments

This study was financed by the Dutch Ministry of Transport and Public Works, National Institute for Coastal and Marine Management/RIKZ, under Contract DGW-996 and the Department of Geochemistry. A. F. Peters is thanked for his contribution to the experimental work, and K. Booij helped with the mathematical formulas. E. H. G. Evers and F. Smedes are thanked for their stimulating contributions to the cosolvent group. J. Kamphuis (Directorate North Sea) and members of the EUZOUT-project provided Atlantic seawater. A. H. M. Harbers helped to improve the manuscript. Two anonymous reviewers are thanked for their useful suggestions. S. M. McNab gave attention to style and language.

Author-Supplied Registry Numbers: Benzo[*a*]pyrene, 50-32-8; phenanthrene, 85-01-8; methanol, 67-56-1.

Glossary

α	empirical constant, eqs 6–8
σ	empirical constant, eqs 6–8
a	empirical constant (eq 9) representing the slope of log K_{oc}* versus $K_S C_{Sal}$
b	empirical constant (eq 9) representing the calculated difference between log K_{oc}* for freshwater and for seawater
f_{oc}	mass-based fraction organic carbon in sediment [(kg of organic carbon) (kg of solid matter)$^{-1}$]
m	suspension concentration, eq 10 (kg L^{-1}) or in text (g L^{-1})
$q_{water,cosolvent}$	molar volume of water or cosolvent (L mol^{-1})
z	volume fraction cosolvent in solution phase
A_L	activity in liquid phase (Bq)
A_S	activity in solid phase (Bq)
C_{Coll}	mass-based component of the apparent concentration associated with colloids [kg (L of water)$^{-1}$]
C_{Coll}*	colloid solution-phase concentration [(kg of colloid) L^{-1}]
C_{DOM}	mass-based component of the apparent concentration associated with DOM [kg (L of water)$^{-1}$]
C_{DOM}*	DOM solution-phase concentration [(kg of DOM) L^{-1}]
C_s	sorbate solid-phase concentration [kg (kg of solid matter)$^{-1}$]
C_{Sal}	molar salt concentration based on NaCl (mol L^{-1}); seawater $\approx$ 0.6 mol L^{-1}
C_w	sorbate true concentration in water [kg (L of water)$^{-1}$]
C'_w	sorbate apparent solution-phase concentration [kg (L of water)$^{-1}$]
K_{Coll}	mass-based partition coefficient between colloids and water [L (kg of colloid)$^{-1}$]
K_{DOM}	mass-based partition coefficient between DOM and water [L (kg of DOM)$^{-1}$]
K_{oc}	organic carbon-normalized partition coefficient
K_{oc}*	organic carbon-normalized partition coefficients derived from K_p* [L (kg of organic carbon)$^{-1}$]
K_{oc}*(sw)	extrapolated organic carbon-normalized partition coefficients in seawater [L (kg of organic carbon)$^{-1}$]
K_{ow}	octanol/water partition coefficient [L (kg of organic carbon)$^{-1}$]
K_p	mass-based true partition coefficient (L kg^{-1})
K_p*	mass-based cosolvent partition coefficient (L kg^{-1})
$\dot{K}_p$	mole-based cosolvent partition coefficient (mol kg^{-1}), eq 8
K_p^{App}	mass-based apparent partition coefficient (L kg^{-1})

$K_{p,m}^{App}$	mass-based sorbate apparent partition coefficient in mixed solvents (L kg^{-1})
$\dot{K}_{p,m}^{App}$	mole-based sorbate apparent partition coefficient in mixed solvents (mol kg^{-1})
K_S	Setschenow constant (L mol^{-1})
S	salinity (g kg^{-1} or ‰)
V_{Total}	total volume of water and cosolvent (L)
$V_{water,cosolvent}$	volume of water or cosolvent (L)

Literature Cited

(1) Grover, R.; Hance, R. J. *Soil Sci.* **1970**, *109*, 136–138.
(2) O'Connor, D. J.; Connolly J. P. *Water Res.* **1980**, *14*, 1517–1523.
(3) Di Toro, D. M.; Horzempa, L. M. *Environ. Sci. Technol.* **1982**, *16*, 592–602.
(4) Horzempa, L. M.; Di Toro, D. M. *Water Res.* **1983**, *17*, 851–859.
(5) Voice, T. C.; Weber, W. J., Jr. *Water Res.* **1983**, *17*, 1433–1441.
(6) Voice, T. C.; Weber, W. J., Jr. *Environ. Sci. Technol.* **1985**, *19*, 789–796.
(7) Resendes, J.; Shiu, W. Y.; Mackay, D. *Environ. Sci. Technol.* **1992**, *26*, 2381–2387.
(8) Wijayaratne, R. D.; Means, J. C. *Environ. Sci. Technol.* **1984**, *18*, 121–123.
(9) Wijayaratne, R. D.; Means, J. C. *Mar. Environ. Res.* **1984**, *11*, 77–89.
(10) Chiou, C. T.; Peters, L. J.; Freed, V. H. *Science* **1979**, *206*, 831–832.
(11) Rebhun, M.; Kalabo, R.; Grossman, L.; Manka, J.; Rav-Acha, Ch. *Water Res.* **1992**, *26*, 79–84.
(12) Chiou, C. T.; Malcom, R. L.; Brinton, T. I.; Kile, D. E. *Environ. Sci Technol.* **1986**, *20*, 502–508.
(13) McCarthy, J. F.; Roberson, L. E.; Burrus, L. W. *Chemosphere* **1989**, *19*, 1911–1920.
(14) Broman, D.; Näf, C.; Rolf, C.; Zebuhr Y. *Environ. Sci Technol.* **1991**, *25*, 1850–1864.
(15) Yalkowsky, S. H.; Valvani, S. C.; Amidon, G. L. *J. Pharm. Sci.* **1976**, *65*, 1488–1494.
(16) Spurlock, F. C.; Biggar, J. W. *Environ. Sci. Technol.* **1994**, *28*, 1003–1009.
(17) Rao, P. S. C.; Hornsby, A. G.; Kilcrease, D. P.; Nkedi-kizza P. *J. Environ. Qual.* **1985**, *14*, 376–383.
(18) Rao, P. S.; Lee, L. S.; Pinal, R. *Environ. Sci. Technol.* **1990**, *24*, 647–654.
(19) Fu, J.-K. A.; Luthy, R. G. *J. Environ. Eng.* **1986**, *112*, 328–345.
(20) Fu, F.-K. A.; Luthy, R. G. *J. Environ. Eng.* **1986**, *112*, 346–366.
(21) Lara, R.; Ernst, W. *Chemosphere* **1989**, *19*, 1655–1664.
(22) Chin, Y. P.; Gschwend, P. M. *Environ. Sci. Technol.* **1992**, *26*, 1621–1626.
(23) Freeman, D. H.; Chueng, L. S. *Science* **1981**, *214*, 790.
(24) McDevit, W. F.; Long, L. A. *J. Am. Chem. Soc.* **1952**, *74*, 1773–1777.
(25) Karickhoff, S. W. *J. Hydraul. Eng.* **1984**, *110*, 707–735.
(26) Harris, L. A.; Bale, A. J.; Bayne, B. L.; Mantoura, R. F. C.; Morris, A. W.; Nelson, L. A.; Radford, P. J.; Uncles, R. J.; Weston, S. A.; Widdows, J. *Ecol. Modell.* **1984**, *22*, 253–284.
(27) Van Zoest, R.; Van Eck, G. T. M. *Neth. J. Sea Res.* **1990**, *26*, 89–96.
(28) Readman, J. W.; Mantoura, R. F. C.; Rhead, M. M.; Brown, L. *Estuarine Coastal Shelf Sci.* **1982**, *14*, 369–389.
(29) Lee, R. F.; Ryan, C. *Can. J. Fish. Aquat. Sci.* **1983**, *40*, 86–94.
(30) Kilroy, A. C.; Gray, N. F. *Water Res.* **1992**, *26*, 887–892.
(31) Walters, R. W.; Guiseppi-Elie, A. *Environ. Sci. Technol.* **1988**, *22*, 819–825.
(32) Brusseau, M. L. *Environ. Sci. Technol.* **1991**, *25*, 1747–1752.
(33) Brusseau, M. L.; Wood, A. L.; Rao, P. S. C. *Environ. Sci. Technol.* **1991**, *25*, 903–910.
(34) Setschenow, J. *Z. Phys. Chem.* **1889**, *4*, 117–125.
(35) Geffcken, G. *Z. Phys. Chem.* **1904**, *49*, 257–302.
(36) Eganhouse, R. P.; Calder, J. A. *Geochim. Cosmochim. Acta* **1976**, *40*, 555–561.
(37) Hermann, R.; Thomas, W. *Fresenius Z. Anal. Chem.* **1984**, *319*, 152–159.
(38) Klamer, J. C.; Laane, R. W. P. M. Presented at the 4th International Conference on Environmental Contamination, Barcelona, 1990, pp 98–100.
(39) Bergen, B. J.; Nelson, W. G.; Pruell, R. J. *Environ. Sci. Technol.* **1993**, *27*, 938–942.

Received for review April 4, 1994. Revised manuscript received November 8, 1994. Accepted November 14, 1994.[⊗]

ES940206Y

[⊗] Abstract published in *Advance ACS Abstracts*, December 15, 1994.